EV's Pulsating Torque Impact On Road-Tire Grip

Chaouachi Taoufik, Lassaad Sbita

Abstract: This paper presents the development of electro-mechanical model of electric ground vehicle, which is equipped with independently actuated in-wheel BLDC motors. Such an electric vehicle (EV) employs in-wheel BLDC motors to independently drive the wheels which is one of the promising vehicle architectures primarily due to its actuation flexibility, energy efficiency, and performance potentials. As known the BLDC has a fluctuation torque where the traditional strategy control for vehicles find to reach the smooth torque [5-10] but the pulsating toque can bring interesting advantage specially to grip the tire to the wet road.

Index Terms: Strategy of control, pulsating torque, grip, slip, in-wheel motor, electric vehicle, Permanent magnetic synchronous motor. Inverter.

1 Introduction

Over the last years, the environmental impact of oil transport, combined with the exhaustion of energy resources, has led to skyrokting the interest of an electric transportion. Electric vehicles differ from fossil fuel vehicles in that the electricity solar and wind energy or any combination of these. The energy consumption of these electric vehicles varies according to the fuel and the technologies used to produce electricity. Electricity can then be stored in the vehicle using an on-board battery[1]. The electric motors are mechanically simple and often achieve high energy conversion efficiencies over the whole range of speed and power developed and can be controlled with high accuracy. Electric motors can be finely controlled and provide high starting torque and do not require multiple gears to match the higher power point.One of most used motor in the BLDC due to high performance and lower cost and the simplicity of control but despite the advantages of the BLDC it has some disadvantages as pulsating torque. In this work, we have supervised the impact of BLDC's inevitable torque fluctuation on the road grip. We attached particular importance to the mechanical transmission system by means of an appropriate modeling of the symbiosis between the electrical management system and the mechanical management system.

2 Electric vehicle model

2.1 Main element of vehicle

The model of the electric vehicle studied is illustrated in figure 2. We focus mainly on the components of the power system that provide electric traction namely[2]:

- The battery,
- The DC/DC converter,
- The inverter,
- In-wheel BLDC,

The battery storage the power in low voltage due to the security and technical constraint. The second element is a DC/DC converter used as a step-up converter used to increase voltage to supply the inverter. Usually several boosts are combined to step up the voltage upstream of the inverter. And finally, the inverter is the final element in the conversion chain which role is to supply the electric engine. The figure 1 present the main element of electric vehicle.

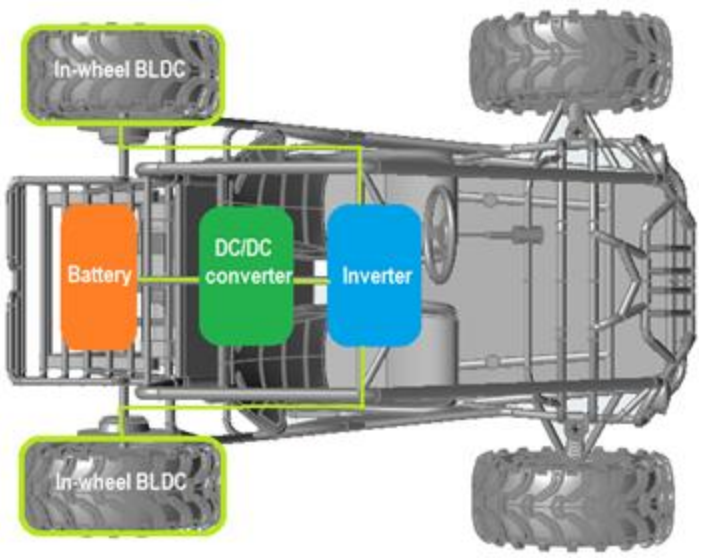

Fig 1:*Rear wheel electric vehicle*

2.2 Battery Model

The charge separation that takes place in each battery cell give rise to a cell voltage, orOpen Circuit Voltage, OCV. As soon as the terminal ends are closed in an electrical circuit,chemical reactions start to take place in the cell, causing the flow of a current. However,due to the charge transport in the electrolyte, and the chemical reactions at the surfaceof the plates and the current in the plates, there is a resistance to the current, which iscalled the battery's internal resistance, R. A simple circuit model of a battery is depicted in Figure 2, where the OCV isdepending on the SOC, and the resistance is constant. There are, however, a number offactors that are not included in this simple model, such as the charge accumulation atthe plates, which gives capacitive contributions to the resistance, SOC and temperaturedependence of all parameters (OCV, R and C), and finally a self-discharge of the battery,that can be modeled as a shunt resistance to the OCV [3].

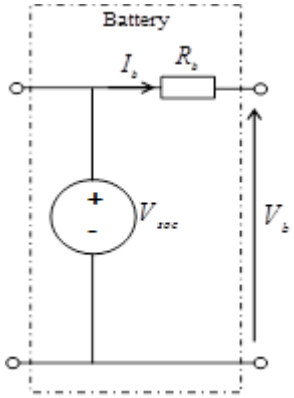

Figure 2:*electrical vehicle battery*

2.3 BOOST CONVERTER MODEL

The energy delivered by the storage battery (V_b, I_b)must meet the requirements DC link voltage level V_{dc} required by the operating point of the BLDC motor [3].

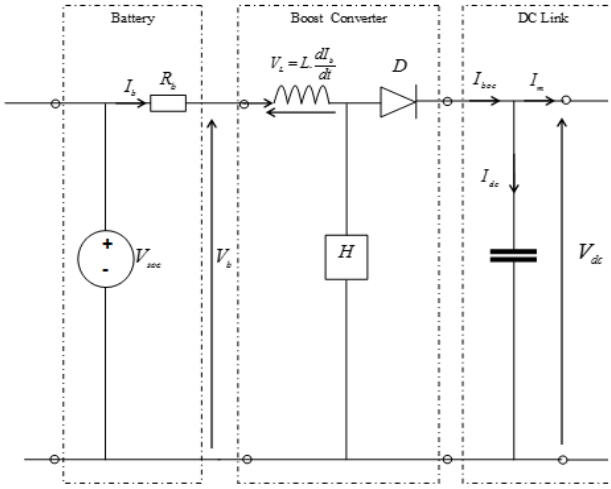

Figure 1: *boost converter*

For these and other reasons, we have integrated a boost (step-up) converter with a duty cycle α_{boc} and a commutation cycle T_{boc} . Referring to the figure 3, we write:

$$V_{dc} = \frac{1}{1-\alpha_{boc}}.V_b \qquad (1)$$

As already reported, Any operating point of the PMSM motor automatically imposes a DC-Link voltage level V_{dc} Therefore, we relied on the control of the duty cycle α_{boc} .

2.4 Model Traction System (inverter and BLDC)

The differential equation model is made for a BLDC motor. The stator winding is a concentrated full-pitch. Three Hall sensors are spaced at 120 degree between each other. Furthermore, the following assumptions are made to build the differential equation of the BLDC motor. the phase voltage of each winding, which includes the resistance voltage drop and the induced EMF. The phase voltage can be presented as

$$u_x = R_x i_x + e_{\Psi_x} \qquad (2)$$

Where
u_x : phase voltage,
i_x: phase current;
e_{Ψ_x} : phase-induced EMF;
R_x: phase resistance.
The winding-induced EMF is equal to the variation rate of the flux. The induced EMF can be written as

$$e_{\Psi x} = \frac{\mathrm{d}\Psi_x}{\mathrm{d}t} \qquad (3)$$

Taking phase, A for example, the flow is given as

$$\Psi_A = L_A i_A + M_{AB} i_B + M_{AC} \mathrm{ic} + \Psi_{pm}(\theta) \qquad (4)$$

Ψ_{pm}: PM flux linkage of phase A;
θ: position angle of rotor, the angle between rotor d-axis and the axis of phase A;
L_A : self-inductance of phase A;
M : mutual inductance of phase A with phase B and phase C.
The magnitude of $\Psi_{pm}(\theta)$ depends on the magnetic distribution in the air gap of the BLDC. The air-gap magnetic field distributes as a trapezoidal profile along the inner surface of the stator, is shown in Figure 4

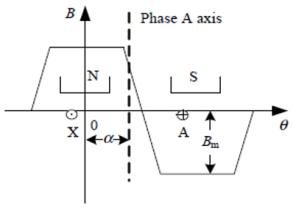

Figure 2: *Flux distribution's BLDC*

As shown in Figure 4, when the rotor rotates, the winding of phase A moves along the y-axis. Then, the effective flux of phase A will change in term of the rotor position. the PM flux of phase A is

$$\phi_{pm} = \int_{-\frac{\pi}{2}+\alpha}^{\frac{\pi}{2}+\alpha} B(\theta) S \,\mathrm{d}\theta \qquad (5)$$

$\phi_{pm}(\alpha)$PM flux of phase A $B(\theta)$ PM rotor radial flux density in the air gap, which is in a trapezoidal distribution[4]. where eA represents the BEMF of phase A. Equation includes a derivative operation of the product of inductance and current, where the self and the mutual inductance of the winding.

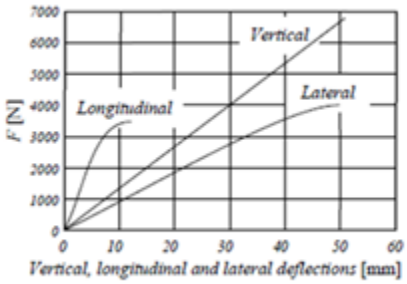

Figure 5:*tire stiffness*

$$u_A = Ri_A + \frac{d}{dt}(L_A i_A + M_{AB} i_B + M_{AC} \mathrm{i}c) + \frac{d}{dt}(NS \int_{-\frac{\pi}{2}+\alpha}^{\frac{\pi}{2}+\alpha} B(\theta)\, \mathrm{d}\theta) \quad (6)$$

$$u_A = Ri_A + \frac{d}{dt}(L_A i_A + M_{AB} i_B + M_{AC} \mathrm{i}c) + e_A \quad (7)$$

Then, the matrix form of phase voltage equation of BLDC motor can be expressed as:

$$\begin{bmatrix} u_A \\ u_B \\ u_C \end{bmatrix} = \begin{bmatrix} R & 0 & 0 \\ 0 & R & 0 \\ 0 & 0 & R \end{bmatrix} \begin{bmatrix} i_A \\ i_B \\ i_C \end{bmatrix} + \begin{bmatrix} L-M & 0 & 0 \\ 0 & L-M & 0 \\ 0 & 0 & L-M \end{bmatrix} \frac{\mathrm{d}}{\mathrm{d}t} \begin{bmatrix} i_A \\ i_B \\ i_C \end{bmatrix} + \begin{bmatrix} e_A \\ e_B \\ e_C \end{bmatrix} \quad (8)$$

The analysis of power and torque for the BLDC motor can be presented as energy transformer from electrical to mechanical. When the motor is operating, the power feeded from the source is absorbed, most of the power caused torque effect. That power called the electromagnetic power which is equals the sum of the product of current and back-EMF of the three phases. That is

$$P_e = e_A i_A + e_B i_B + e_c i_c \quad (9)$$

Ignoring the mechanical loss and stray loss, the electromagnetic power is totally turned into kinetic energy, so:

$$P_e = T_e \Omega \quad (10)$$

Where T_e electromagnetic torque and Ω angular velocity of rotation. we can get:

$$T_e = \frac{e_A i_A + e_B i_B + e_c i_c}{\Omega} \quad (11)$$

A great deal of study has been devoted to identifying the sources, characteristics, and minimization of torque ripple [5]–[10].In order to build a complete mathematical model of the electromechanical system, the motion equation has to be included as

$$T_e - T_L = J\frac{\mathrm{d}\Omega}{\mathrm{d}t} + B_v \Omega \quad (12)$$

3 TIRE DYNAMICS

Before starting in the tire dynamics we must reveal that the tire is directly mounted on the in-wheel BLDC of electric vehicle. Now in tire dynamics the tire is the main element with its interaction with the road. The performance of a vehicle is mainly influenced by the characteristics of its tires. The tires affect the maneuverability, traction, ride comfort and fuel efficiency of the vehicle.

3.1Tire stiffness

The deformation behavior of the tires at the forces applied in three directions x, y and z are the dynamic principal characteristics of the tire. The calculation of tire stiffness is mainly based on experiments, they depend on the mechanical properties of the tire. Consider a tire loaded vertically on a floor. The tire will deform under load and generate pressure in the contact area to balance the vertical load. Figure 5 illustrates a sample of the experimental stiffness curve at (Fz, Δz). The curve can be expressed by a mathematical function.

$$F_z = f(\Delta_z) \quad (13)$$

However, a linear approximation can be applied.

$$F_z = \frac{\partial f}{\partial \Delta z} \Delta z \quad (14)$$

The coefficient ∂f/∂ (Δz) is the slope is the slope of the experimental stiffness curve at zero which represents a stiffness coefficient k_z.

$$k_z = \lim_{\Delta z \to 0} \frac{\partial f}{\Delta z} \quad (15)$$

After approximation, the vertical force of the tire k_z can be calculated as a linear function of the normal deflection of the tire Δz measured at the center tire.

$$F_z = k_z \Delta z \quad (16)$$

3.2 Rolling resistance

When a tire turns on the road, part of the circumference of the tire passing on the road is compressed, so some of the energy spent on deformation will not be restored during the next relaxation. Therefore, a change in the distribution of the contact pressure makes the normal stress [11]σz in the upstream part of the tire footprint is greater than the downstream part. The dissipated energy and the distortion of the stress present cause the rolling resistance.

Figure 6 illustrate a normal tire stress distribution σz and the resulting force Fz for a rotating tire. Due to the normal stress which is higher in the front part of the tire footprint, the resulting normal force is slightly ahead in the center which generates a moment of resistance in the opposite direction of the movement which opposes the rotation in rotation. Dividing the resistance moment by the radius of the wheel will obtain a longitudinal fictitious force called rolling resistance [12] present in equation 16.

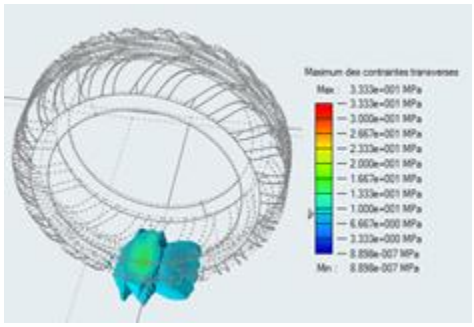

Figure 6: *normal wheel impression stress*

$$F_r = \frac{1}{R_h} M_r = \frac{\Delta_x}{R_h} F_z \qquad (17)$$

A tire that rotates on the ground generates a longitudinal force called rolling resistance. The force is opposed to the direction of movement and is proportional to the normal force that causes the tire footprint.

$$F_r = \mu_r F_z \qquad (18)$$

The parameter μ_r is the coefficient of friction of rolling. μr mainly depends on tire speed, inflation pressure, skid angle and incline angles which depends on mechanical properties, speed, temperature, load, driving and braking forces and road condition. the rolling coefficient of friction depends on speed, inflation pressure and load, skid angle and camber angle. Rubber tires generate friction according to two mechanisms, adhesion and deformation, as presented in equation.

$$\mu_r = \mu_{de} + \mu_{ad} \qquad (19)$$

The adhesion friction μ_{ad} occurs as a result of the molecular bond between rubber and surfaces. The high pressure due to the wheel / road contact creates a molecular bond. This bonding occurs at the contact points and glues the surfaces together. The deformation friction μ_{de} is the result of the deformation of the tire due to hysteresis and the road profile. A higher deformation friction increases therefore increases the frictional force. Deformation friction exists in the relative motion[13-14] between each surface contact. In case of wet road μ_{ad} reach the zero and the electric vehicle slips.

4 Simulation An d Result

*The electric vehicle (fig 7) is composed from two rear wheel drive. The vehicle has those characteristics: Sprung mass 400k_g, Roll inertia 440 $k_g m^2$, Pitch inertia 1343 $k_g m^2$, Yaw inertia 1343 $k_g m^2$. μ_{ad} =0.2. The two BLDC motors have those parameter Rs=1.15 , Ls= 0.0025 H,Ke=1.46 Nm / A.

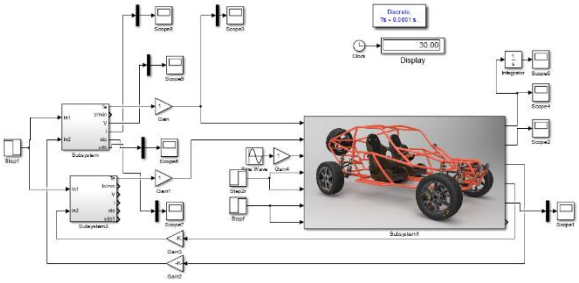

Figure 7: *Two BLDC Rear wheels vehicle*

After simulation we observe in figure 8 and figure 11 the vehicle lost the contact with road due to the low adhesion. The Figure 9 and 10 represent respectively the torque and BEMF.

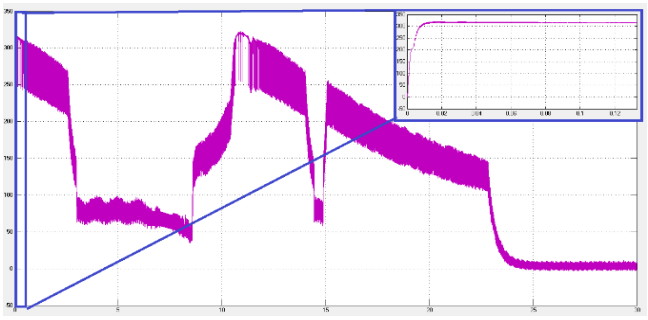

Figure 8:*Slip of vehicle on road*

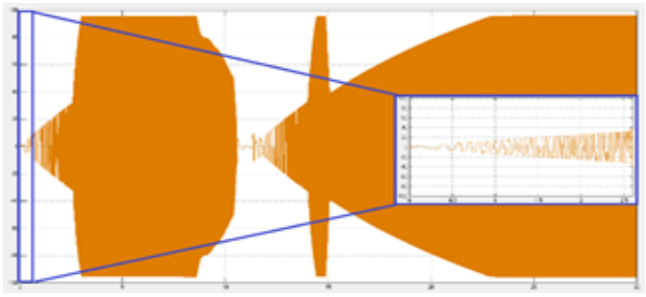

Figure 9:*The torque of BLDC (sliped vehicle)*

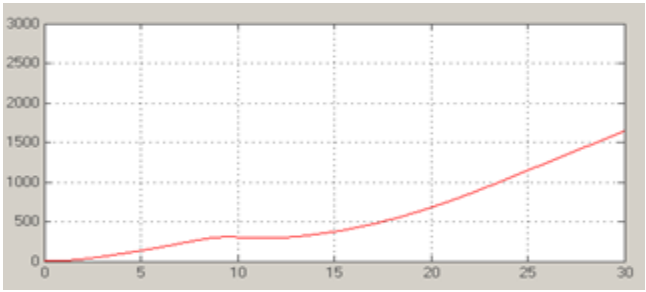

Figure 10:*The BEMF of BLDC (sliped vehicle)*

As presented in figure 9 the torque is smooth as almost strategy of BLDC control [5-10] then the deformation friction μ_{de} is very low then the total friction will be close to zero. After adopting new strategy of control to tolerate a fluctuation torque seen in figure 12 the vehicle displaces without any slip as presented in figure 13 and the BEMF is presented in figure 14.

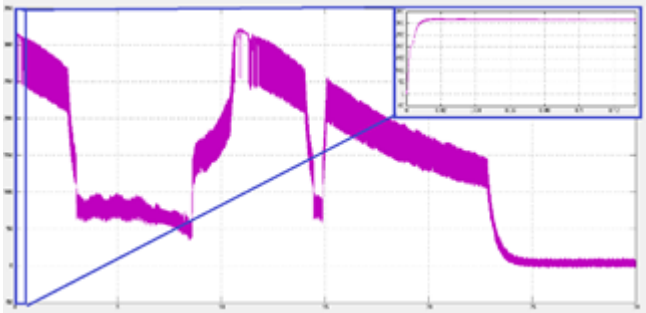

Figure 11:*Displacement of sliped vehicle*

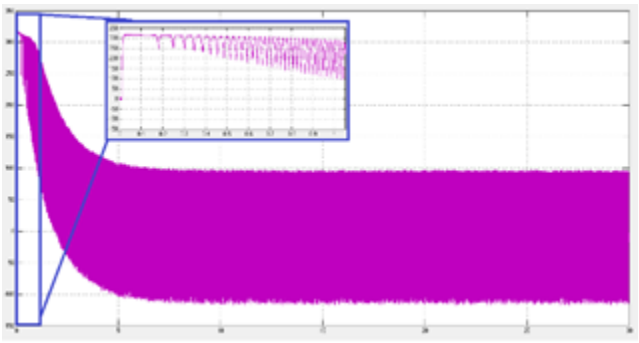

Figure 12: *Flucutation torque of EV's BLDC*

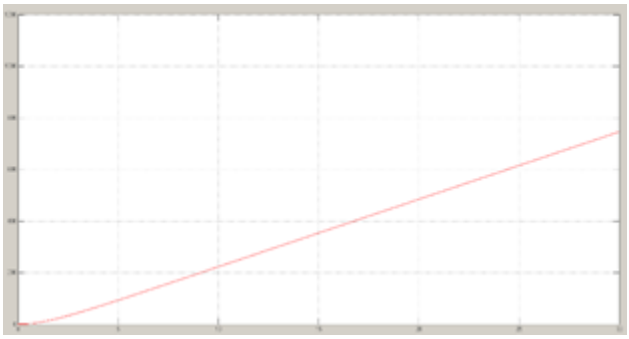

Figure 13: *Dispalcement of vehicle based on new strategy*

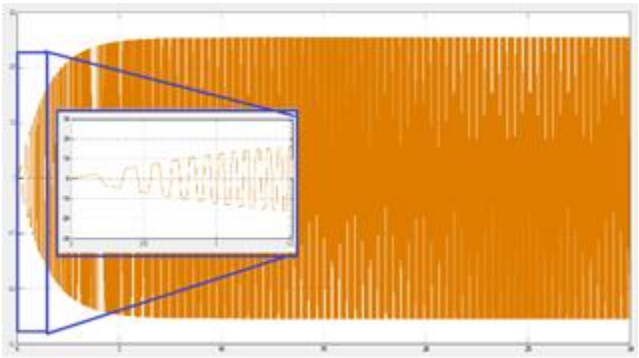

Figure 14: *The BLDC's BEMF of new strategy*

5 CONCLUSIONS

In this work, we are interested in the effect of electric vehicle torque on the slip between velicule wheel and the wet road. we can say that the design and optimization of the traction chain of an electric vehicle is a multidisciplinary problem that must taken by consideration. That multidisciplinary system puches as to devlop the tire dynamics whitch revel the importance of tire stiffness, rolling resistance and the friction. The deformation is one kind of friction which can be caused by micro hyterisis of tire due to pulsating torque. That deformation friction can help the electric vehicle to grip on the road.

REFERENCES

[1] CONTROL SYSTEMS FOR HIGH PERFORMANCE ELECTRIC CARS PEDRET Paula, WEBB Jonathan, , BAYONA Guillermo, MOURE Christophe, BOLTSHAUSER Sandro Volume 6 - Issue 1 - Pages 88-94.

[2] IMPACT OF ELECTROMOBILITY ON AUTOMOTIVE ARCHITECTURES LUCCARELLI Martin, RUSSO SPENA Pasquale, MATT Dominik Volume 6 - Issue 1 - Pages 1-8, World Electric Vehicle Journal Vol. 6 - ISSN 2032-6653 - © 2013 WEVA .

[3] Intelligent Control Of An Electric Vehicle, Taoufik Chaouachi, Kamel Jemaï, INTERNATIONAL JOURNAL OF SCIENTIFIC & TECHNOLOGY RESEARCH VOLUME 6, ISSUE 01.

[4] Xinghua Wang, Qingfu Li, Shuhong Wang, & Qunfeng Li. (2003). Analytical calculation of air-gap magnetic field distribution and instantaneous characteristics of brushless dc motors. IEEE Transactions on Energy Conversion, 18(3)

[5] T. M. Jahns, "Torque production in permanent magnet synchronous motor drives with rectangular current excitation," IEEE Trans. Ind. Applicat., vol. 20, pp. 803–813, July/June 1984

[6] H. R. Bolton and R. A. Ashen, "Influence of motor design and feedcurrent waveform on torque ripple in brushless DC drive," Proc. Inst. Elect. Eng., vol. 131 B, no. 3, pp. 82–90, May 1984

[7] D. Hanselman, J. Y. Hung, and M. Keshura, "Torque ripple anaysis in brushless permanent magnet motor drive," in Proc. ICEM'92, Manchester, U.K., Sept. 1992, pp. 823–827.

[8] H. Le-Huy, R. Perret, and R. Feuillet, "Minimization of torque ripple in brushless DC motor drive," IEEE Trans. Ind. Applicat., vol. 22, pp. 748–755, July/Aug. 1986.

[9] J. Y. Hung and Z. Ding, "Minimization of torque ripple in permanent magnet motors," in Proc. 18th IEEE Industrial Electronics Conf., San Diego, CA, Nov. 1992, pp. 459–463.

[10] D. C. Hanselman, "Minimum torque ripple, maximum efficiency excitation of brushless permanent magnet motors," IEEE Trans. Ind. Applicat., vol. 41, pp. 292–300, June 1994.

[11] Bay, N., & Wanheim, T. (1976). Real area of contact and friction stress at high pressure sliding contact. Wear, 38(2), 201–209.

[12] Ono, E., Hattori, Y., Muragishi, Y., & Koibuchi, K. (2006). Vehicle dynamics integrated control for four-wheel-distributed steering and four-wheel-distributed traction/braking systems. Vehicle System Dynamics, 44(2), 139–151.

[13] Padmanabhan, V., & Laursen, T. A. (2001). A framework for development of surface smoothing procedures in large deformation frictional contact analysis. Finite Elements in Analysis and Design, 37(3), 173–198.

[14] Greenwood, J. A., Minshall, H., & Tabor, D. (1961). Hysteresis Losses in Rolling and Sliding Friction. Proceedings of the Royal Society A: Mathematical, Physical and Engineering Sciences, 259(1299), 480–507.